CHARACTERIZE BY DRX, UV VIS, ET AFM. THIN FILM DIOXYDE TITANIUM

A. Besbes [1*], A. Beniaiche [2]

[1]1 *Institute of physic, Department of physic, UFAS of Sétif, Algeria*
[2] *Institute of optic and mechanic of precision, UFAS, Sétif, Algeria*
** besbesmoetacim@yahoo.fr*

Keywords: Semiconductor thin film TiO_2-Ag solar energy.

Abstract
Energy is a huge question in this 21st century; the ability to solve energy problems today is the ability to solve most of the ills and sufferings of our societies. The decrease in inventories of crude oil, global warming and air pollution associated with the use of hydrocarbons show the need to consider alternative sources of energy and abundant renewable.
Titanium dioxide (TiO_2) is widely used in various industries (cosmetics; painting; solar cells; used-water reprocessing; electro-chromatic systems; etc.). It exists under different crystalline forms: rutile, anatase, and brookite. We have prepared our samples using an alcoholic solution of Isopropoxyde of titanium. The solution thus prepared by a sol–gel method on a soda-lime glass substrate. The layers undergo a heat treatment at temperatures varying from 500 with 600°C, and various dippings. DRX analysis of our thin films of TiO_2 shows that the titanium oxide starts to crystallize starts from the temperature of annealing 500°C.

1 Introduction

Transparent conducting oxide coatings are important element in a large number of applications, due to the unique combination of high electrical conductivity with good optical transmission in the visible range [1]. In recent years, titanium dioxide has been extensively used as an environmentally harmonious and clean photocatalysts, because of its various qualities, such as optical properties, low cost, high photocatalytic activity, chemical stability and non-toxicity [2].

Crystalline TiO_2 film exist in three phases: anatase (tetragonal), rutile (tetragonal), and brookite (orthorhombic), rutile being the most stable of the three, and the formation of its phase depending on the starting material, deposition method and temperature treatment. In particular, TiO_2 thin films can transform from amorphous phase into crystalline anatase and from anatase into rutile by changing temperature. In this semiconductor material, the absorption of ultraviolet light energy h = Eg (Eg of TiO_2 = 3.2eV), this corresponds to a wavelength between 360-380nm, results in the production of electron pairs - hole. [3].

2 Materials

2.1 *Preparation of the solution and deposition of the layer*

In this work we prepared two types of layers: a layer of TiO_2, the other layer doped by silver (Ag-TiO_2 with different percentage of Ag).

2.1.1 Preparation of the solution of TiO_2

The chemical process of gelation of a sol-gel film involves several steps: Pour 1 ml of titanium isopropoxide in a beaker. Adding 2 ml of isopropanol, and mixed for 10 min. adding 0.3ml of acetic acid (mixed for 15 min). Finally we add 10 ml of methanol and mixed the soil for one hour.

2.1.2 *Preparation of the solution of Ag-TiO_2*

We conducted the following procedure: A mixture of 0.2 g of silver nitrate, 20 ml of nitric acid (mixture for 10 min), with the previous solution (mixture for 10 min).

2.1.3 Deposition of the layer

The method we used in this study is the dip-coating to increase the thickness of the layer is deposited samples several times, in this case is deposited samples after three time, five and eight times. The heat treatment in this study separated into two stages followings:

A) Drying: For the development of our layers, we carried out 20 minutes of drying at 150 ° C in an oven to bake after waiting a few minutes for the more volatile products have evaporated.

B) Annealing: TiO_2 thin amorphous films can be formed at low temperatures between 100 ° - 150 ° C. Amorphous TiO_2 do not have a strict crystallographic structure, the crystalline phase of the lowest temperature of TiO_2 can be achieved is anatase. For the anatase polycrystalline film can be deposited as amorphous TiO_2 and then be crystallized by annealing at high temperature for this work we chose a temperature of 500 ° C.

2.2 *Characterizations*

Film morphology was characterized by Atomic Force Microscope. The crystalline phases and crystallite size of TiO_2 was studied by XRD technique. The X-ray diffraction patterns were obtained on a D8 Advanced Bruker X-ray diffractometer using Cu Kα radiation at an angle of 2θ from 15 to 60°. The scan speed was 1^o/min. The strongest peaks of TiO_2 corresponding to anatase (101) was selected to evaluate the crystallinity of the samples. The mean crystallite size L was determined from the broadening β of the most intense line, for each polymorph, in the X-ray diffraction pattern, based on the Scherer equation [2,4,5,6]:

$$L = \frac{0.9\lambda}{\Delta(2\theta)cos\,\theta} \quad (1)$$

With:
L = average crystallite size in Å.
λ = wavelength of the excitation line (1.54098 Å).
θ= Bragg angle corresponding to the position of the line.
Δ(2θ) = width at half height of the line considered.

UV-vis (spectrophotometer calculate the index of refraction, by envelope method, and to deduce the optical gap of the layer. The UV–visible spectra from our samples are obtained using a SHIMADZU 1700 double–beam spectrophotometer controlled by computer.

3. Result and discussion

3.1 XRD Analysis.

The crystalline phase of the powders that evolved after Annealing was examined by XRD D8 Advanced Bruker X-ray diffractometer using Cu Kα irradiation (λ = 0.154056 nm) at 45 kV and 40 mA radiation at an angle of 2θ from 15 to 60°. The crystallite size (D) was estimated from the width of lines in the XRD pattern according to the Scherrer equation. The XRD patterns of film of TiO_2 Annealing at 450◦C were showed in Figure 1.

The spectra provide information on the distances d hkl of different families of planes (hkl) in the sample and thus the crystalline phase. From the Figure 1 we see that the beginning of crystallization of the anatase phase from 500 ° C.

3.1.1 The film annealed at 500 ° C

• 5 layers: the XRD diffraction pattern shows a peak around 25.35 ° a distance d hkl = 3.5115 A ° to the plane (101), crystallite size L = 31.34 nm.

• 8 layers: the XRD diffraction pattern shows several peaks for the (101) around the angle of 25.15 ° the distance between the plane are 3.5403 A ° to the plane (101), crystallite size is 8.7 nm. For other peaks are the crystallite size 25.1 nm and 32.5 following nm corresponds to the following plans (004) to 37.9 ° and the angle (200) to the angle 48.2 °, respectively.

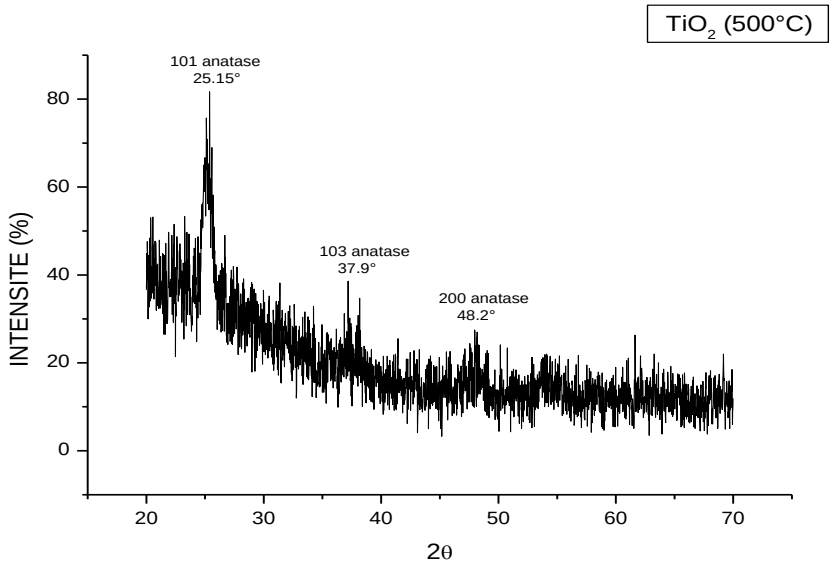

Figure 1 : The evolution of diffraction spectra, film annealed at 500°C.

3.1.2 The film annealed at 600 ° C

Well crystallized layer, the XRD diffractogram shows several peaks for the (101) around the corner of 25.01° the distance between the plane are 3.5598 A° to the plane (101), crystallite size is 24.33nm. For other peaks we determined the size of anatase nanocrystals 31.11 16.29 16.70 and 17.45nm in the directions normal to the planes, respectively (112) at 2θ = 38.05°, (200) at 2θ = 48.63° (211) to 2θ = 54.45 and (204) at 2θ = 63.34°.

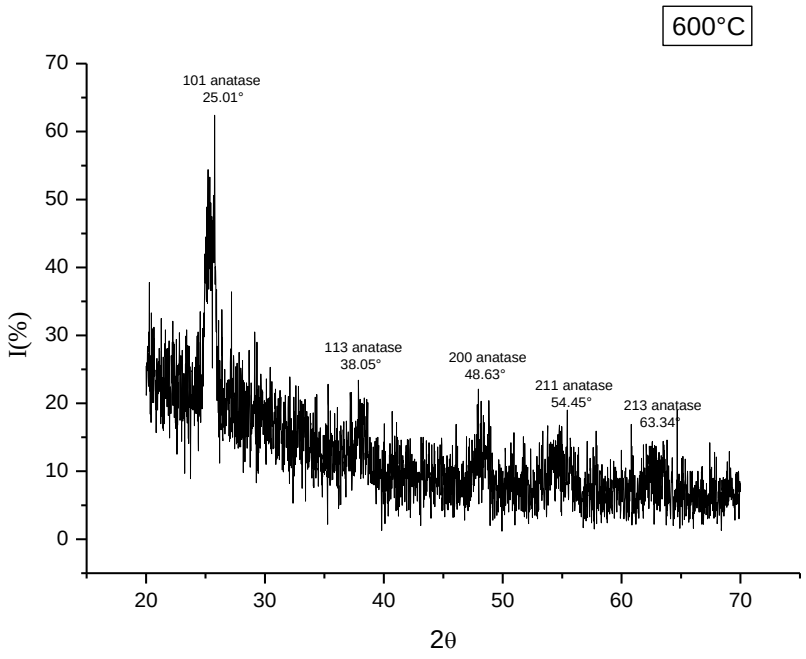

Figure 2: The evolution of diffraction spectra. Film annealed at 600°C.

The texture coefficient (*TC*) represents the texture of a particular plane, whose deviation from unity implies the preferred growth. Quantitative information concerning the preferential crystallite orientation was obtained from another texture coefficient TC (hkl) defined as [6]:

$$TC(hkl) = \frac{\frac{I(hkl)}{I_0(hkl)}}{\sum_n \frac{I(hkl)}{I_0(hkl)}} \times 100\% \qquad (3)$$

Where I (hkl) is the measured relative intensity of a plane (hkl) and I_0 (hkl) is the standard intensity of the plane (hkl) taken from the JCPDS data. The value TC (hkl) = 1 represents films with randomly oriented crystallites, while higher values indicate the abundance of grains oriented in a given (hkl) direction. The specific surface area of the sample was calculated from the formula (2) [7]:

$$S = 6 \times \frac{10^3}{\rho d} \qquad (2)$$

Where, S is the specific surface area ($m^2\ g^{-1}$), d is the average crystallite size, and ρ (g/cm^3) is the density of anatase or rutile (3.85 and 4.25 g/cm^3, respectively) [7].

The variation of *TC* for the peaks is presented in Table 1 and 2.

hkl	**d_{hkl}**	**2θ (°)**	**d(nm)**	**s (m^2**	**TC[%]**
101	3.5403	25.15	8.7	179.13	35.05
004	2.3786	37.9	25.1	62.08	33.18
200	1.8869	48.2	32.5	48.07	31.77

Table 1: Results for film annealed at 500°C.

hkl	**d_{hkl} (A)°**	**2θ (°)**	**d(nm)**	**s (m^2 g^{-1})**	**TC[%]**
101	3.560	25.01	24.33	64.05	23.22
004	2.3737	37.87	11.31	137.79	7.14
200	1.8722	48.63	16.29	95.66	18.21
211	1.6849	54.45	16.70	93.31	28.21
204	1.4683	63.34	17.45	89.30	23.22

Table 2: Results for film annealed at 600°C.

3.2 UV-Vis Analysis. We find that undoped samples exhibit a high transmittance (> **65-85%,** depending on thickness) in the visible range. The observed oscillations are the result of interference at the interfaces air-film and film-substrate. They are characteristic of a high index material, deposited on a support of low index. This is the case of anatase (**n=2.5)** on soda-lime glass **(n=1.513).** The amplitude of the oscillations decreases with increasing film thickness. In addition, the transmittance maximum at **450-500 nm**, decreases the thickness of the layer thickness goes. This is a consequence of light scattering which increases with the roughness and the anisotropy resulting from the increase in grain size. see figure 3(a).

For samples doped found low transmission below **λ = 350 nm** due to absorption in the UV TiO_2 matrix. The comparison between the graph transmission of undoped films with graph of doped films shows that there is a significant absorption between 350 nm and 475 nm with a maximum around 405 nm. Or chute transmission. See figure 3(b).

The refraction indices *n* at various wavelengths were calculated using the envelope curve for T_{max} (T_M) and T_{min} (T_m) in the transmission spectra. The expression for the refractive index is given by [1,8,9]:

$$n = \left[N + (N^2 - n_s^2)^{1/2}\right]^{1/2} \qquad (2)$$

$$N = 2n_s \frac{T_m - T_M}{T_m T_M} + \frac{n_s^2 + 1}{2} \qquad (3)$$

Where n_s are the refractive index of the medium soda-lime glass (1.513), T_m and T_M are the maximum and minimum transmittances at the same wavelength.

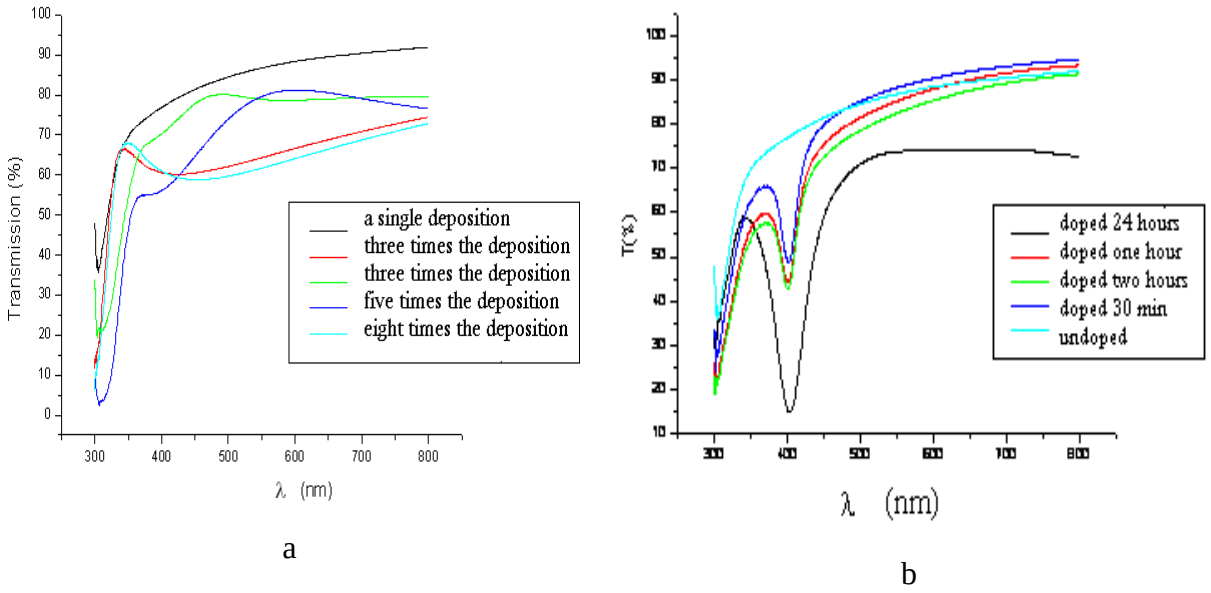

Figure 3: transmission spectrum: (a) undoped film, (b) doped film.

The thickness is calculated by this equation:

$$d = \frac{M\lambda_1\lambda_2}{2[\lambda_2 n(\lambda_1) - \lambda_1 n(\lambda_2)]} \quad (4)$$

Where M is the number of oscillations between the minimum and maximum choice (M = 1 between two consecutive minima and maxima) and λ_1, λ_2 and n (λ_1), n (λ_2) wavelengths and indices corresponding refraction.

The results also show the evolution of the index n as a function of layer thickness. Index increased slightly from 1.78 in 2.269 when the thickness decreases from 761 nm to 309 nm. See table.

Thickness (nm)	**Réfractive index n(λ)**		**Porosity (%)**
316	2.236 (λ=345 nm)	2.146 (λ=425 nm)	10.3 15.07
309	2.269 (λ=350 nm)	2.155 (λ=445 nm)	8.83 14.43
574	2.059 (λ=360nm)	1.988 (λ=410nm)	19.35 21.97
761	1.78 (λ=488nm)	1.760 (λ=588 nm)	34.56 35.27

Table 3: Evolution of index.

The absorption coefficient follows a variation with the energy type[9,10]:

$$(\alpha h\nu) = B\left(h\nu - E_g\right)^m \qquad (6)$$

Figure (4) shows the variation of the root of the absorption coefficient is multiplied by the energy hv, according to the energy *hv*. Between field of fundamental absorption, which corresponds to high energies, and the field stabilization energies corresponding to low, in this graph there are part linear variation, by extrapolating this part α = 0, there is a decrease in the optical gap when the thickness is increased, the optical gap is 3.05 for a thickness of 761 nm for layers undoped.

Figure(5): a decrease in the band gap around 2.7eV (for 2 hours) to 2.58 eV (for 24 hours), due to the presence of silver.

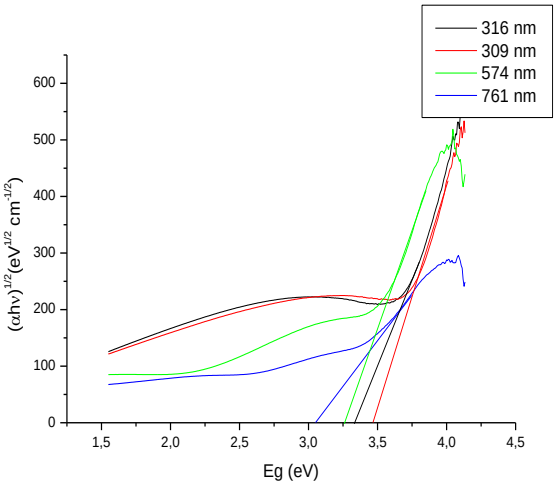

Figure 4: Variation of $(\alpha h\nu)^{1/2}$ as a function of *hv*.

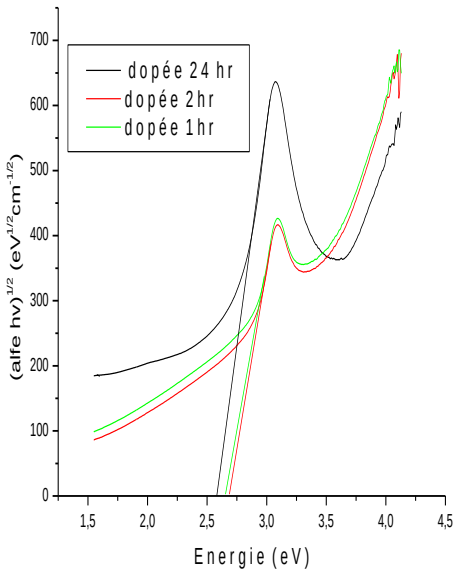

Figure 5: Determination of the gap of Ag-TiO_2.

From the gap we can calculate the carrier concentration of the doped layer. Using the following equations [11]:

$$\Delta E_g = \frac{h^2}{8em^*}\left(\frac{3N10^6}{\pi}\right)^{2/3} \quad (7)$$

$$N^{2/3} = \frac{\Delta E_g}{2.77 * 10^{-16}} \quad (8)$$

ΔEg [eV] : widening of the gap to the Burstein-Moss effect.
N [cm^{-3}]: carrier concentration.
m^*: effective mass of electron

Electrons in TiO_2 have a very large effective mass (~10 m_e or more) [12].

Time of doped the layer	**N (carrier concentration) Unité 10^{21} cm^{-1}**
one hour	13.4
Two hours	15.5
24 hours	18.5

Table 3: Evolution of carrier concentration by time of doping.

3.3 *AFM Analysis:* TiO_2 grains is very crystallized and oriented, the grain size is estimated around 100 nm for undoped layers. The observation of AFM images indicated an increase in porosity when the thickness becomes thick. TiO_2 grains disappeared by the effect of the presence of silver.
The size of grains silver estimated around 5nm-10nm, so it is difficult to capture by force atomic microscope.

Roughness:

For 100nm thick found an average roughness of Ra = 2.90nm. For Ra = 309nm 4nm thick.
For 761nm thick = 3 nm Ra.
For the doped layer we find a mean roughness Ra = 2.70nm.

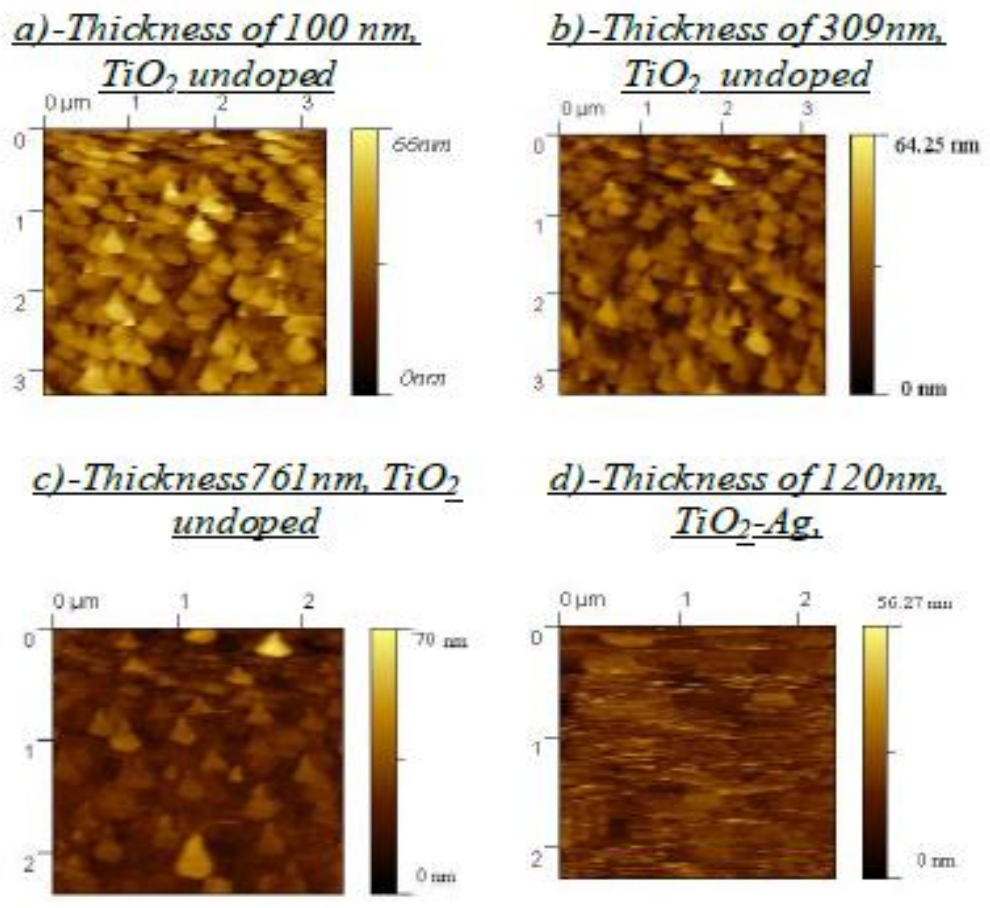

Figure 1: AFM imagerie.

4. Conclusion

We determined the crystallite size anatase in the direction normal to the planes (101) (103) and (200), the crystallite size was estimated between 10 and 35nm. For samples prepared at 500 ° C, we determined the crystallite size of anatine in the direction normal to the planes (101) (112) (200) (211) and (204), the crystallite size was estimated between 11 nm and 25 nm.

For undoped layers we see an optical gap around 3.2 eV, the index decreases when the thickness becomes thick. For the doped layers there is a change in gap at 3.2eV (2.58 eV) for Ag-TiO_2.

References

[1]M. Nocuń and Z. Pająk, "The influence of glass surface preparation on electrical and optical properties of SnO2 thin films obtained by spray pyrolysis technique", Optica Applicata, Vol. XXXVIII, No. 1, 2008, pp. 181–187.

[2]Lek Sikong, Budsabakorn Kongreong,Duangporn Kantachote and Weerawan Sutthisripok, "Photocatalytic Activity and Antibacterial Behavior of Fe^{3+}-Doped TiO_2/SnO_2 Nanoparticles", Energy Research Journal 1 (2): 120-125, 2010.

[3]F. Laura Toma, Nadine Keller, Ghislaine Bertrand, Christian Coddet and Didier Klein**,** "Elaboration et caractérisation des propriétés environnementales de dépôts de dioxyde de titane obtenus par projection thermique", Thème of congres, Tours, Matériaux, 2002.

[4]M. Nasr-Esfahani and M. Hossein Habibi, "Silver doped TiO_2 nanostructure composite photocatalysts film synthesized by sol-gel spin and dip coating technique on glass", International Journal of Photoenergy, Volume 2008, Article ID 628713.

[5]R. Jourdani, A. Outzourhit, A. Oueriagli, D. Aitelhabti,E. L. Ameziane, S. Barazzouk and S. Hotchandani "Structural, optical and electrochromic properties of nanocrystalline TiO_2 thin films prepared by spin coating",Active and Passive Electronic Components, September 2004, Vol. 27, pp. 125–131.

[6]S. Ilican, M. Caglar, Y. Caglar," Determination of the thickness and optical constants of transparent indium-doped ZnO thin films by the envelope method", Materials Science-Poland, 2007 Vol. 25, No. 3,pp. 709-718.

[7]M.R. Mohammadi, M.C. Cordero-Cabrera, D.J. Fray and M. Ghorbani, "Preparation of high surface area titania (TiO_2) films and powders usingparticulate sol–gel route aided by polymeric fugitive agent", Sensors and Actuators B, Vol. 120, (2006), pp. 86–95.

[8]R. Palomino-Merino, A. Conde-Gallardo, M. Garcia-Rocha, I. Hernandez-Calderon, V. Castano and R. Rodriguez, "Photoluminescence of TiO_2: Eu^{3+} thin films obtained by sol-gel on Si and Corning glass substratesThin", Solid Films 401 (2001), pp. 118-123

[9]M. A. Ben Said, S. Belgacem, M. Dachraoui, R. Bennaceur and H. Bouchriha;" Caractérisations structurale et optique de bicouches $Cd_{1-y}Zn_yS$/CuPc : mise en évidence d'un effet photovoltaïque", Revue Phys. Appl. 21 (1986), vol. 07, pp. 407-415

[10] Junyong Kang, Shin Tsunekawa and Atsuo Kasuya, "Ultra violet absorption spectra of SnO_2 nanocrystallites, Applied Surface Science 174(2001), pp. 306-309.

[11]R. Chowdhury, P.Rees, S.Adhikari, F.Scarpa and S.P.Wilks," Electronic structures of silicon doped ZnO", Physica B, Vol. 405, (2010), pp. 1980–1985.

[12]R. Chowdhury, P.Rees, S.Adhikari, F.Scarpa and S.P.Wilks," Electronic structures of silicon doped ZnO", Physica B, Vol. 405, (2010), pp. 1980–1985.